

NUMERICAL STUDY FOR THE PARAMETER ESTIMATION OF THE MOISTURE TRANSFER COEFFICIENT : 2D CASE

YONG HUN LEE* AND YEON HEE PARK

ABSTRACT. The thermal behavior of wood exposed to the outdoors is influenced by solar absorptivity and longwave emissivity. However, it is difficult to measure that properties directly. Hence we estimate the values of the parameter by using the least-square optimization technique. Finally we report the results for the computation of the values of the parameters.

AMS Mathematics Subject Classification : 76S05, 65C20, 80A20, 74G15.

Key words and phrases : parameter estimation, moisture transfer coefficient, solar absorptivity, emissivity, Gauss-Newton method.

1. Introduction

The governing equations to represent the moisture and thermal behavior of wood are known by coupled heat and mass equations defined as

$$a_1 \frac{\partial m}{\partial t} = \nabla \cdot (k_{11} \nabla m + k_{12} \nabla T) \quad (1.1)$$

$$a_2 \frac{\partial T}{\partial t} = \nabla \cdot (k_{21} \nabla m + k_{22} \nabla T), \quad (1.2)$$

where m and T represent the moisture contents and thermal temperature, respectively. Also, the distribution of the moisture contents and temperatures are determined by boundary conditions. Recently, there are few results [5, 6, 7] for various type of the boundary conditions. For examples, for the case of kiln drying, the effect of the drying at the external surface depends only on the dry and web bulb temperature of the kiln.

$$\begin{aligned} k_{11} \nabla m + k_{12} \nabla T &= h_c (\rho_{\infty, v} - \rho_v) \\ k_{21} \nabla m + k_{22} \nabla T &= h_T (T - T_{\text{dry}}) + h_c \Delta h_v (\rho_v - \rho_{\infty, v}), \end{aligned}$$

where h_c and h_T are external convective mass and heat transfer coefficients, respectively, ρ_v and $\rho_{\infty, v}$ are water vapor density at the wood surface and of

Received April 7, 2011. Revised June 7, 2011. Accepted June 10, 2011. *Corresponding author.
© 2011 Korean SIGCAM and KSCAM.

surrounding air, respectively and T and T_{dry} are the temperature at the wood surface and of dry bulb, respectively, and Δh_v is the latent heat of evaporation. In the kiln drying, the T_{dry} and $\rho_{\infty, v}$ is settled by the temperature of bulb and relative humidity of the kiln.

For the case of indoors, the effect of the drying at the external surface depends on the relative humidity and temperature of the air.

$$\begin{aligned} k_{11}\nabla m + k_{12}\nabla T &= h_c(\rho_{\infty, v} - \rho_v) \\ k_{21}\nabla m + k_{22}\nabla T &= h_T(T - T_\infty) + h_c\Delta h_v(\rho_v - \rho_{\infty, v}), \end{aligned}$$

where T_∞ are the temperature of surrounding air. In this case, the T_∞ and $\rho_{\infty, v}$ are fluctuated and calculated by the temperature and the relative humidity of the air.

For the case of outdoors, the process of the drying at the external surface is influenced on the solar radiation as well as air temperature and relative humidity of air. Material properties include solar absorptivity and longwave emissivity. Hence the boundary conditions are represented as

$$\begin{aligned} k_{11}\nabla m + k_{12}\nabla T &= h_c(\rho_{\infty, v} - \rho_v) \\ k_{21}\nabla m + k_{22}\nabla T &= h_T(T - T_\infty) + h_c\Delta h_v(\rho_v - \rho_{\infty, v}) - q_{r, \text{net}}, \end{aligned}$$

where $q_{r, \text{net}}$ is the net solar radiance. The net solar radiance can be expressed by using the solar absorptivity and emissivity which are the material properties of the wood.

Knowledge of the thermal behavior of wood exposed to the outdoors is important for assessing the durability and expected performance of any exterior wooden component. Furthermore, thermal behavior also affects moisture transfer, and, hence, plays an important role in determining the moisture gradient in wood. The thermal performance of exterior wood depends on the outdoor environment, as well as on intrinsic material properties. Material properties include solar absorptivity and longwave emissivity. However, there are few studies available on the solar absorptivity and longwave emissivity of wood species because direct measurement on the broadband frequency range is difficult, especially in case of emissivity. Hence, in this paper, we investigate the estimation of the value of solar absorptivity and emissivity by the least-square approximation which compares the numerical solution and experimental data of the moisture contents and the temperature of wood species. Therefore, this study is conducted to estimate solar absorptivity and longwave emissivity indirectly using the inverse method after measuring the surface temperature of some wood species horizontally exposed to an outdoor environment.

In section 2, we introduce the governing equations for the process of heat and mass transfer, the numerical method for solving this differential equations, control volume finite element method and the methods of the parameter estimation is introduced in section 3. Finally, we report the computational results.

2. Formulation of the Heat and Mass Transfer Equation

We consider the coupled heat and mass transfer equations with two state variables of moisture content m and temperature T which can be represented as follows:

$$\rho_{ow} \frac{\partial m}{\partial t} = \nabla \cdot (k_{11} \nabla m) + \nabla \cdot (k_{12} \nabla T) \tag{2.3}$$

$$\rho C_p \frac{\partial T}{\partial t} = \nabla \cdot (k_{21} \nabla m) + \nabla \cdot (k_{22} \nabla T) \tag{2.4}$$

where ρ and ρ_{ow} are the density of the raw and oven-dried wood, respectively, and C_p is the specific heat of wood. The coefficients k_{ij} are functions of moisture contents m and temperature T . Here the density and the specific heat are represented as [4],

$$\rho = \frac{\rho_{ow}(1 + m)}{1 + m\rho_{ow}/1000}$$

$$C_p = \frac{103.1 + 3.867T + 4190m}{1 + m} + m(-6191 + 23.6T - 1330m).$$

In this paper, we consider the outdoor weather condition to the air temperature, relative humidity and solar radiation, regardless the rain drop and the wind speed. Hence the boundary equations at exposed surfaces are given as following:

$$-k_{11} \nabla m - k_{12} \nabla T = h_c(\rho_{\infty,v} - \rho_v) \tag{2.5}$$

$$-k_{21} \nabla m - k_{22} \nabla T = h_T(T_s - T_\infty) + h_c \Delta h_v(\rho_v - \rho_{\infty,v}) - q_{r,net}, \tag{2.6}$$

where h_c and h_T are external convective mass and heat transfer coefficients, respectively, and ρ_v and $\rho_{\infty,v}$ are water vapor density at the wood surface and of surrounding air, respectively and T_s and T_∞ are the temperature at the wood surface and of surrounding air, respectively, and Δh_v is the latent heat of evaporation and $q_{r,net}$ is the net solar radiance.

The net solar radiance $q_{r,net}$ can be expressed by the following equation [3],

$$q_{r,net} = \alpha G - \varepsilon \sigma (T_s^4 - T_{sky}^4), \tag{2.7}$$

where α and ε are the solar absorptivity and emissivity, respectively and G is incident solar radiance and T_s and T_{sky} is the temperature at the wood surface and of sky, respectively. T_{sky} is the equivalent blackbody sky temperature, defined to be the equivalent temperature of the clouds, water vapor, and other atmospheric elements that make up the sky to which a surface can radiate heat. Sky temperature is an important parameter for calculating radiative heat transfer between an object at a given temperature above absolute zero ($0^\circ K$) and the sky.

The fictive sky temperature depends on the exterior air temperature, humidity, and cloudiness. For a partially overcast sky it may be estimated by the equation by Cole [2].

$$T_{sky} = T_a [\varepsilon_0 + 0.84c(1 - \varepsilon_0)]^{0.25} \tag{2.8}$$

where T_a is the exterior air temperature, ε_0 is the emissivity of the clear sky and c is the fractional cloud cover.

Berdahl and Martin [1] proposed an equation for the emissivity of a clear sky depending on the dew point and time in relation to midnight.

$$\varepsilon_0 = 0.711 + 0.0056T_{dp} + 0.000073T_{dp}^2 + 0.013 \cos(2\pi \frac{n}{24}) \quad (2.9)$$

where T_{dp} is the ambient dew point and n is the time until or since midnight in hours ($0 \leq n \leq 24$). For dew points between $-20^\circ C$ and $30^\circ C$, this equation is valid only for clear sky conditions. The difference between air and sky temperature is from $5^\circ K$ in a hot and moist climate to $30^\circ K$ in a cold and dry climate.

$$p_{vs} = \exp\left(23.5771 - \frac{4042.9}{T_a - 37.58}\right) \quad (2.10)$$

$$p_v = p_{vs} \times \varphi \quad (2.11)$$

$$T_{dp} = 37.58 - \frac{4042.9}{\log p_v - 23.5771} \quad (2.12)$$

where p_{vs} is the saturated water vapor pressure, p_v is the water vapor pressure and φ is the relative humidity.

By replacing the expression of the density of water vapor into moisture content, the boundary equations (2.5)-(2.6) may be rewritten as:

$$-k_{11}\nabla m - k_{12}\nabla T = h_m(m_\infty - m) \quad (2.13)$$

$$-k_{21}\nabla m - k_{22}\nabla T = h_T(T_\infty - T) + h_m\Delta h_v(m_\infty - m) - q_{r,net} \quad (2.14)$$

where h_m and h_T are the external convective mass and heat transfer coefficients, respectively, and satisfies the following relation:

$$h_m = h_c \frac{M_v p_{vs,\infty}}{RT} \frac{\partial h}{\partial m}. \quad (2.15)$$

The two convective transfer coefficients are dependent each other if the Prandtl and Schmidt numbers, or the thermal and water vapor diffusivities are equal. If the Nusselt and Sherwood numbers would be equal and the Lewis number equals to unity, leading to the Lewis relation:

$$h_c \cong \frac{h_T}{\rho_a C_{pa}}. \quad (2.16)$$

Therefore, a convective mass transfer coefficient can be evaluated from convective heat transfer coefficients that are more established from the literature data.

To predict the radiation on a vertical or column surface, it should be known to be the direct, diffuse and reflected radiation. However, measurement data usually give the total radiation only on the horizontal surface.

According to Reindl et al. [8, 9], The horizontal diffuse radiation depends on the ambient temperature and the relative humidity as well as the sky clearness, which can be estimated from the total radiation on the horizontal surface.

3. Parameter Estimation

In this section, we introduce the numerical method to estimate the value of the parameters using the least square methods and the control volume finite element methods. In order to determine the values of the parameters $P = [p_1, p_2, \dots, p_n]$ of diffusion equations and boundary conditions, we define the objective functional to be minimized as follows:

$$F(P) = \sum_{j=1}^m |T(t_j) - T_e(t_j)|^2, \tag{3.17}$$

where $T(t_j)$ and $T_e(t_j)$ is the computational temperature and experimental temperature at the certain point after t_j seconds, respectively.

In this paper, three columns of species were used in this experiment, which were air-dried in the indoor environment for more than a half-year and to about 12% moisture content. The wood columns with dimension of $2.4m \times 0.2m \times 0.2m$ were cut into three in length of $0.7m$. The average density of wood columns was $437kg/m^3$, ranged from $424kg/m^3$ to $455kg/m^3$.

The top and bottom of wood columns were insulated by aluminum foil and Styrofoam. For measuring thermal and moisture content changes, the columns were exposed to outdoor weather conditions for one day, 15 May 2008. The column was placed in four cardinal directions. The field test was conducted at Chonnam National University, located at Gwangju in Korea. K type of thermocouples was used for measuring the temperatures of surface which has a full south aspect and midpoint. Temperatures were set to be data-logged automatically at one minute interval. The profile of the temperature of 3 columns of species during a one day are depicted in Figure 1. Figure shows that there contains some experimental error.

The necessary condition to minimize the function at P^* is

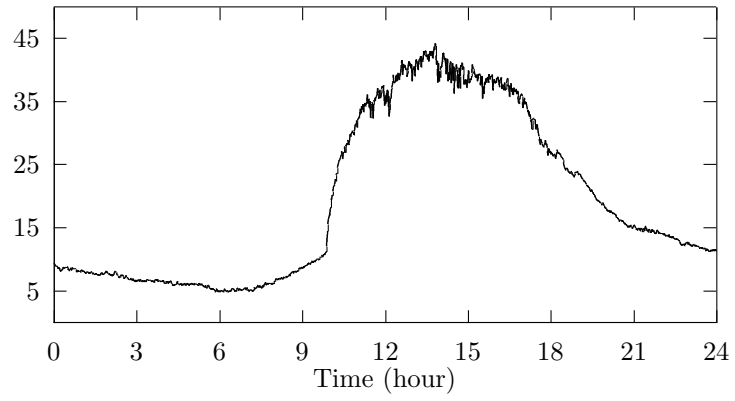
$$\nabla F(P^*) = 0.$$

Then the gradient of $F(P)$ is

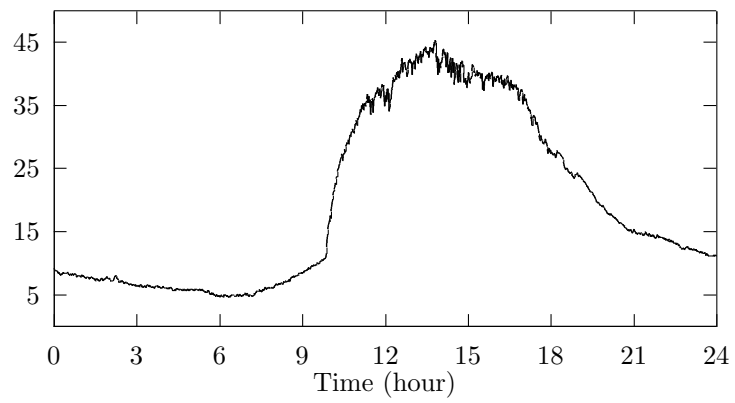
$$\nabla F(P) = \sum_{j=1}^m r_j(P) \nabla r_j(P) = J(P)^T r(P),$$

where $r(P) = (r_1, r_2, \dots, r_m)^T$, and

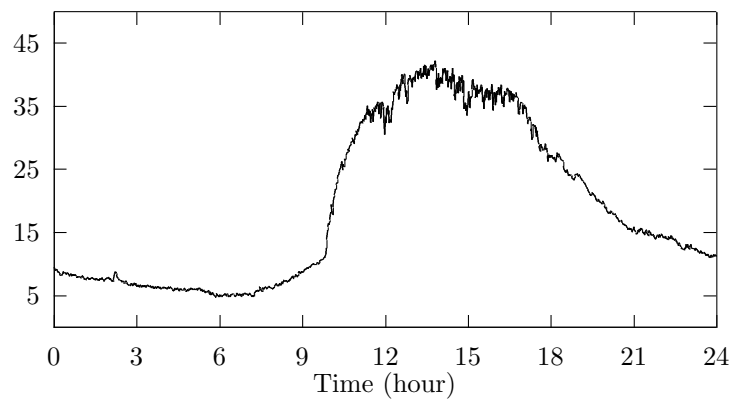
$$r_j(P) = |T(t_j) - T_e(t_j)|, \quad j = 1, \dots, m,$$



(a) Sample 1



(b) Sample 2



(c) Sample 3

FIGURE 1. The profiles of the temperature at surface

and the Jacobian matrix $J(P)$ of $r(P)$ is

$$J(P) = \begin{pmatrix} \frac{\partial r_1}{\partial p_1} & \frac{\partial r_1}{\partial p_2} & \cdots & \frac{\partial r_1}{\partial p_n} \\ \frac{\partial r_2}{\partial p_1} & \frac{\partial r_2}{\partial p_2} & \cdots & \frac{\partial r_2}{\partial p_n} \\ \vdots & \vdots & \ddots & \vdots \\ \frac{\partial r_m}{\partial p_1} & \frac{\partial r_m}{\partial p_2} & \cdots & \frac{\partial r_m}{\partial p_n} \end{pmatrix},$$

where the partial derivatives $\frac{\partial r_j}{\partial p_i}$ is approximated by discrete formula as following:

$$\frac{\partial r_j}{\partial p_i} = \frac{r_j(P + h\mathbf{e}_i) - r_j(P - h\mathbf{e}_i)}{2h}, \tag{3.18}$$

where \mathbf{e}_i is unit vector which only has 1 at i -th component and $h > 0$ is small quantity. However, this system of equations is nonlinear and difficult to compute. Hence the Newton's method is used to solve this system. The original Newton's iterative formula has the form.

$$P^{(k+1)} = P^{(k)} - \left[J(P^{(k)})^T J(P^{(k)}) + S(P^{(k)}) \right]^{-1} J(P^{(k)})^T r(P^{(k)}),$$

where Hessian $S(P)$ has the second-order derivative such as

$$S(P) = \sum_{j=1}^m r_j(P) \nabla^2 r_j(P).$$

However, second-order derivative term is expensive to compute and make the system ill-conditioned. Hence, by neglecting this second-order term in Newton's method, the simplified iteration is the following Gauss-Newton iteration

$$P^{(k+1)} = P^{(k)} - \left[J(P^{(k)})^T J(P^{(k)}) \right]^{-1} J(P^{(k)})^T r(P^{(k)}). \tag{3.19}$$

These parameters were adjusted by the fitting procedure until the best agreement between experimental and simulation was obtained.

In order to find the computational temperature we use discretization method so called the control volume finite element method(CVFEM). Now, we introduce CVFEM which is used to discretize our diffusion equations. We recast coupled heat and mass transfer equations to typical formulation as following:

$$\frac{\partial}{\partial t} \Psi + \nabla \cdot \mathbf{J} = 0, \tag{3.20}$$

where Ψ represents the quantities with state variables $\rho_{ow}m$ or $\rho C_p T$ and the fluxes \mathbf{J} represents

$$\begin{aligned} \mathbf{J}_w &= k_{11} \nabla m + k_{12} \nabla T, \\ \mathbf{J}_e &= k_{21} \nabla m + k_{22} \nabla T, \end{aligned}$$

respectively. Applying time discretization technique such as the backward Euler to (3.20), we have the following stationary equation at each time step

$$(\Psi - \Psi^{(\text{prev})})/\delta t + \nabla \cdot \mathbf{J} = 0, \quad (3.21)$$

where $\Psi^{(\text{prev})}$ means the value of the quantity Ψ at the previous time step. δt means the time step size. As shown as Figure 2, the computational domain is meshed with triangular elements, and at each node the control volumes (CVs) are constructed. One sees the technique adopted in this paper for constructing the CVs around the element vertices.

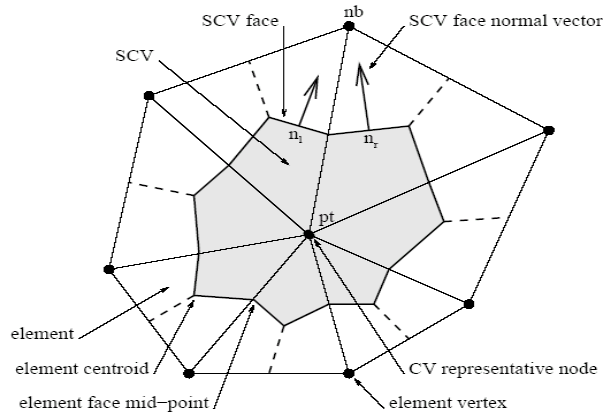


FIGURE 2. Construction of a two-dimensional control volume (shaded region) consisting of sub-control volumes.

To obtain the discretized formulation of the stationary equation (3.21), we have integrating over the each CV

$$\frac{\text{Area}(\text{CV})}{\delta t} (\Psi_{\text{pt}} - \Psi_{\text{pt}}^{(\text{prev})}) + \int_{\text{CV}} \nabla \cdot \mathbf{J} dS = 0,$$

where Ψ_{pt} , the value of Ψ at the node point pt , is representative value of Ψ in the CV, i.e.,

$$\Psi_{\text{pt}} = \frac{1}{\text{Area}(\text{CV})} \int_{\text{CV}} \Psi dS,$$

and applying the Gauss divergence theorem:

$$\alpha \Psi_{\text{pt}} - \sum_{f \in \mathfrak{F}_{\text{CV}}} (\mathbf{J} \cdot \mathbf{n})_f = \alpha \Psi_{\text{pt}}^{(\text{prev})},$$

where $\alpha = \frac{\text{Area}(\text{CV})}{\delta t}$, \mathfrak{F}_{CV} is the set of faces enclosing the CV and \mathbf{n}_f is outward normal vector with size of the length of face. Also the term $(\mathbf{J} \cdot \mathbf{n})_f$ is evaluated accurately at the midpoint of the face.

In order to evaluate to approximated flux at the face of the CV, we use finite element shape functions for the diffusion terms. Then we have the $3N$ discrete analogue of the equations (3.21) as following:

$$F_{pt}(x) := \alpha(\Psi_{pt}^{(n+1)} - \Psi_{pt}^{(n)}) - \sum_{f \in CV} ((\alpha_1 \mathbf{J}_{pt}^{(n+1)} + \alpha_2 \mathbf{J}_{nb1}^{(n+1)} + \alpha_3 \mathbf{J}_{nb2}^{(n+1)}) \cdot \mathbf{n})_f = 0,$$

where the superscript $(n+1)$ means the current time level $t^{(n+1)}$, (n) the previous time level $t^{(n)}$, and time step size is $\delta t = t^{(n+1)} - t^{(n)}$.

Now, we introduce the iterative algorithm to estimate the parameters. At first step, we choose the initial guess $P^{(0)} = [p_1^{(0)}, p_2^{(0)}, \dots, p_n^{(0)}]$. Then we can calculate the numerical solution of the heat and mass equations for the values of the parameters $P^{(0)}$ by using control volume finite element methods and also obtain the value of the objective functional (3.17). Since the value of the objective functional may be not the minimum value, for the next step, we can find the values of the next step $P^{(1)}$ from the iterative equation (3.19). For the purpose of it, we must find the Jacobian matrix $J(P^{(0)})$, i.e., we have to compute the approximated value (3.18) of the partial derivative $\frac{\partial r_j}{\partial p_i}$. Hence for the values of the parameters $P^{(0)} \pm h\mathbf{e}_i = [p_1^{(0)}, \dots, p_i^{(0)} \pm h, \dots, p_n^{(0)}]$, $(i = 1, 2, \dots, n)$, we obtain the values of the objective functional. Until the minimum value of the functional is obtained, we repeat the iterative process. Then we can get the values of the parameters which the functional is minimized.

4. Numerical Results

In this section, we report numerical simulation results. In order to discretize for the control volume finite element method, the rectangular samples of wood were meshed with a triangular elements. The density of wood were assumed to be $400kg/m^3$. Convective heat and mass transfer coefficients were assumed to be $h_T = 10W/m^2K$ and $h_m = 0.0025m/s$. The convective coefficients are given to be as following.

$$\begin{aligned} k_{11} &= 7 \times 10^{-2} e^{1000(m-4)/RT} \\ k_{22} &= 7 \times 10^{-1} e^{100(m-12)/RT}. \end{aligned}$$

In this calculation, the k_{12} and k_{21} are neglected. For numerical differential, we may assume $h = 10^{-7}$. For the parameter estimation, we use two parameters, i.e., the solar absorptivity α and the longwave emissivity ε are setting to the parameter p_1 and p_2 . For the Gauss-Newton iteration, the initial guess for the values of α and ε , we take $\alpha = 0.8$ and $\varepsilon = 0.5$ for the three samples, respectively. The results of Gauss-Newton iteration are shows in Table 1. After $6 \sim 8$ iteration, we obtain the minimal value of the objective functional $F(P)$. The profile of the temperature at the initial guess ($\alpha = 0.8$ and $\varepsilon = 0.5$) and the final profile of the temperature of the minimal value which are compared with the experimental data are depicted for the three samples in Figure 3.

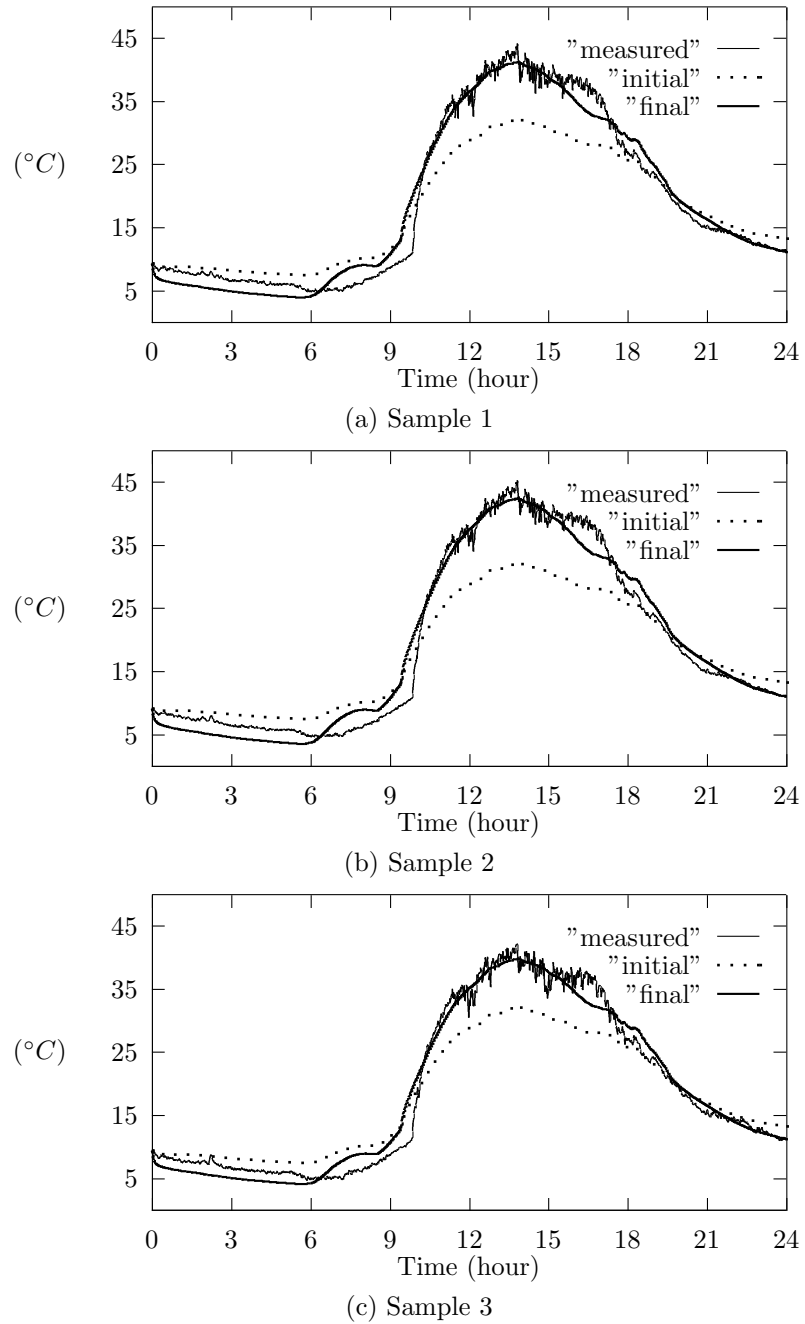


FIGURE 3. The profiles of the temperature at surface

n	α	ε	$F(P)$
0	0.800000	0.500000	34410.111298
1	1.104833	0.753371	8173.279037
2	0.990811	0.679504	6351.316789
3	0.939754	0.643632	6298.086673
4	0.937863	0.642271	6297.058186
5	0.940100	0.643799	6297.020707
6	0.939344	0.643261	6297.014585

(a) Sample 1

n	α	ε	$F(P)$
0	0.800000	0.500000	43005.564803
1	1.115566	0.759372	13928.831652
2	1.009180	0.690918	7024.626625
3	0.955323	0.651281	6767.634999
4	0.955865	0.650892	6760.633622
5	0.956326	0.650953	6760.357789
6	0.956087	0.650714	6760.347828
7	0.956309	0.650838	6760.346692
8	0.956646	0.651075	6760.346286

(b) Sample 2

n	α	ε	$F(P)$
0	0.800000	0.500000	26522.946286
1	0.974551	0.690664	9791.558504
2	0.892916	0.632368	5507.029406
3	0.864383	0.608929	5327.290125
4	0.874541	0.615191	5320.101069
5	0.876226	0.615997	5319.751237
6	0.876873	0.616340	5319.739136
7	0.876023	0.615715	5319.732121
8	0.876074	0.615751	5319.732107

(c) Sample 3

TABLE 1. The computational results of Gauss-Newton iteration

5. Concluding Remark

It is important to know the solar absorptivity and the longwave emissivity of the wood. But it is difficult to measure this material property. Using the nonlinear least-square method and control volume finite element method for the heat and mass equation, we estimate the value of the parameters, the solar absorptivity and the longwave emissivity, by inverse technique.

However, the error analysis and the convergence analysis of the iterative scheme has not been achieved. For further study, we want to establish the theoretical theory for the convergence and error analysis.

REFERENCES

1. P. Berdahl and M. Martin, *Emissivity of clear skies*, Solar energy, **32** No. 5 (1984), 663-664.
2. R. J. Cole, *The longwave radiation incident upon the external surface of buildings*, The Building Service Engineer, **44** (1976), 195-206.
3. J. A. Duffie and W. A. Beckman, *Solar Engineering of Thermal Processes. 2nd Ed*, John Wiley and Sons Inc., New York, 1991.
4. Forest Products Laboratory, *Wood Handbook. Wood as an engineering material*, General technical report FPL GTR-113, USDA Forest Service, Forest Products Lab., Madison, 1999.
5. W. Kang, Y. H. Lee, W. Y. Chung and H. L. Xu, *Parameter estimation of moisture diffusivity in wood by an inverse method*, J. of wood sciences, **55** (2008) 83-90.
6. Y. H. Lee, *Numerical solution for the parameter estimation of the moisture transfer coefficients*, Honam Mathematical Journal, **32** No. 2 (2010) 193-202.
7. Y. H. Lee, W. Kang and W. Y. Chung, *Numerical solution for wood drying on one-dimensional grid*, J. Korean Society for Industrial and Applied Mathematics, **11** No. 1 (2007) 95-105.
8. D. T. Reindl, W. A. Beckman and J. A. Duffie, *Diffuse fraction correlations*, Solar Energy, **45** (1990) 1-7.
9. D. T. Reindl, W. A. Beckman and J. A. Duffie, *Evaluation of hourly tilted surface radiation models*, Solar Energy, **45** (1990) 9-17.
10. C. Skaar, *Wood-water relations. p210*, Springer-Verlag 1988.
11. C. Tremblay, A. Cloutier and Y. Fortin, *Experimental determination of the convective heat and mass transfer coefficients for wood drying*, Wood Sci. Technol. **34** (2000), 253-276.
12. I. W. Turner and P. Perré, *The use of implicit flux limiting schemes in the simulation of the drying process*, Applied Mathematical Modelling, **25** (2001), 513-540.

Yong Hun Lee received M.Sc. from Yonsei University and Ph.D. at KAIST. Since 1997 he has been at Chonbuk National University. His research interests include numerical optimization and partial differential equations.

Department of Mathematics, Institute of Pure and Applied Mathematics, Chonbuk National University, Jeonju 561-756, Korea.

e-mail: lyh229@jbnu.ac.kr

Yeon Hee Park received M.Sc. and Ph.D. from Yonsei University. Since 1982 she has been at Chonbuk National University. Her research interests are integration, optimization and analysis.

Department of Mathematics Education, Institute of Pure and Applied Mathematics, Chonbuk National University, Jeonju 561-756, Korea.

e-mail: yhpark@jbnu.ac.kr